Magnetic Resonance in Medicine 43:295–302 (2000)

In Vivo Intravoxel Incoherent Motion Measurements in the Human Placenta Using Echo-Planar Imaging at 0.5 T

R.J. Moore,[1] B. Issa,[1] P. Tokarczuk,[1] K.R. Duncan,[2] P. Boulby,[1] P.N. Baker,[2] R.W. Bowtell,[1] B.S. Worthington,[1] I.R. Johnson,[2] and P.A. Gowland[1]*

This paper presents the first in vivo measurements of intravoxel incoherent motion in the human placenta, obtained using the pulsed gradient spin echo (PGSE) sequence. The aims of this study were two-fold. The first was to provide an initial estimate of the values of the IVIM parameters in this organ, which are currently unknown. The second aim was then to use these results to optimize the sequence timings for future studies. The moving blood fraction (f), diffusion coefficient (D), and pseudo-diffusion coefficient (D*) were measured. The average value of f was 26 ± 6 % (mean ± SD), D was 1.7 ± 0.5 × 10^{-3} mm^2/sec, and D* was 57 ± 41 × 10^{-3} mm^2/sec. For the optimized values of b, the expected percentage uncertainty in the fitted values of f, D, and D* for the placenta were $\sigma f/f$ = 14.9%, $\sigma D/D$ = 14.3%, $\sigma D^*/D^*$ = 44.9%, for an image signal-to-noise of 20:1, and a total imaging time of 800 sec. Magn Reson Med 43:295–302, 2000. © 2000 Wiley-Liss, Inc.

Key words: IVIM; human placenta; EPI; optimization; PGSE

This work aims to demonstrate the ability of magnetic resonance imaging to make noninvasive in vivo measurements of intravoxel incoherent motion (IVIM) in the placenta (1). Pilot data has been acquired and has then been used to optimize the sequence for use in any future studies. This work forms part of a project to determine the potential of echo-planar magnetic resonance imaging (EPI) in assessing the compromised fetus. Intrauterine growth restriction (IUGR) is a major cause of perinatal mortality and morbidity. Pregnancies complicated by IUGR are known to be associated with defective trophoblastic invasion during placental development, which impedes uteroplacental blood flow. It is expected that blood movement measurements made using this technique will eventually provide a method for probing placental structure and function, with the aim of assisting in the prediction of IUGR.

There has been much deliberation over the interpretation of IVIM measurements, in particular over the link between IVIM and classical perfusion (2,3,4). Classical perfusion is a measure of the blood delivered to and used by a specified mass of tissue, and is measured in units of ml/min/100 g. It is often measured using spin labelling techniques in MRI (5). In contrast, IVIM measures quasi random blood movement within a single imaging voxel and results in a bi-exponential signal attenuation in a standard pulsed gradient spin echo (PGSE) experiment. The pseudo-diffusion coefficient (D*) is associated with perfusion and is measured in units of mm^2/sec. Signal attenuation due to D* is observed at lower values of b as it relates to larger scale movement. The affects of diffusion, quantified by the diffusion coefficient (D) and also measured in units of mm^2/sec, are observed at higher values of b and are related to smaller scale movement of water (6). The value of f measures the total volume of blood moving in the voxel compared to the total voxel volume and is quoted as a percentage.

The PGSE sequence (7) has previously been used to measure f, D, and D*, predominantly in the brain where it has been criticized for its low sensitivity (8). However, the expected volume of moving blood in the placenta is high, reducing image signal-to-noise requirements and improving sensitivity to f and D*, suggesting that the placenta would be an ideal site in which to use this sequence.

The development of obstetric MRI has been hampered by the presence of motion artifacts in images of the fetus. The unpredictable and nonperiodic nature of fetal movement makes it impossible to use simple techniques such as gating or retrospective gating to reduce these artifacts. However, it is possible to produce good quality images of the fetus using high-speed imaging techniques such as EPI (9), FLASH (10), or HASTE (11) to freeze physiological motion. A further advantage of high-speed imaging is that it provides a method of obtaining quantitative results in a reasonable imaging time, thereby minimising patient discomfort or stress, which is particularly important when scanning pregnant subjects. EPI takes 130 msec to form an image as implemented here (approximate echo train length), with an echo time to the origin of *k*-space of 35 msec. It is ideally suited to imaging the fetus because it produces minimal RF power deposition. Furthermore, despite the sensitivity of EPI to variations in magnetic susceptibility, there are no significant image artifacts in fetal imaging because the susceptibility of the fetus is well matched to the uterine environment.

In order to produce meaningful quantitative results *in vivo* using MRI, the measurement parameters must always be chosen to maximize the reproducibility of the measured values. This is particularly important in this study because pregnant subjects cannot lie comfortably in the scanner for long periods and the work is conducted at low field strength. Therefore, it is important to select the optimum combination of diffusion sensitivity or b values to maximize the reproducibility in f, D, and D*. The measure-

[1]Magnetic Resonance Centre, School of Physics and Astronomy, University of Nottingham, UK.

[2]Obstetrics and Gynaecology, City Hospital, University of Nottingham, UK.

Dr. B. Issa's present address is Department of Physics, P.O. Box 17551, UAE University, Al-Ain, United Arab Emirates.

Dr. P. Tokarczuk's present address is Imaging Science and Biomedical Engineering, University of Manchester, Manchester, UK.

Dr. P. Boulby's present address is MR Centre, National Society for Epilepsy, Chalfont St. Peter, Buckinghamshire SL9 ORJ, UK.

This work was presented at the 5th Meeting of the ISMRMB in Vancouver, April 1997.

*Correspondence to: Dr. P. A. Gowland, Magnetic Resonance Centre, University of Nottingham, Nottingham NG7 2RD, UK.

Received 17 July 1998; revised 18 October 1999; accepted 19 October 1999.

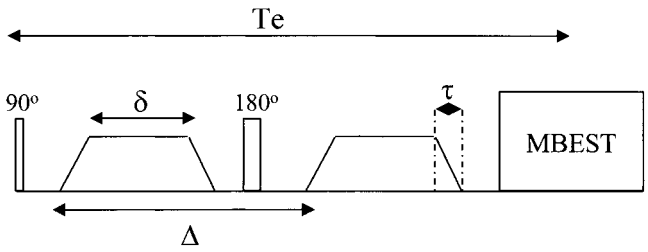

FIG. 1. Schematic diagram of the PGSE sequence.

ments reported here were acquired using an unoptimized sequence to provide an indication of the true values of f, D, and D* in the human placenta in vivo. They have subsequently been used to optimize the PGSE sequence specifically for the placenta, so that more reproducible results can be obtained in the future. Details of the optimization methods and results are also presented.

EXPERIMENTAL METHODS

Subjects

Approval for this study was obtained from the ethics committee of The City Hospital, Nottingham. IVIM measurements were obtained for 11 women with apparently normal healthy pregnancies. The gestational age ranged from 20 weeks to term, the average being 30 weeks (SD = 6 weeks). The work reported here forms part of a larger project studying the use of EPI in the assessment of the compromised fetus, and one aim of this was to monitor fetal organ growth (12). Therefore, at each scanning session, an initial multi-slice data set was collected to locate the placenta, assess its orientation, and allow the future calculation of placental and other organ volumes. This was followed by IVIM measurements of the placenta using the PGSE sequence, and sometimes various other quantitative MRI measurements.

Magnetic Resonance Scanning

All scanning was performed on the 0.5 T purpose built echo-planar imaging scanner at the University of Nottingham. The MBEST (9) echo-planar encoding sequence was used, with the switched gradient sinusoidally modulated at 0.5 kHz. The in-plane resolution was 3.5 mm × 2.5 mm (switched × broadening gradient), the slice thickness was 7 mm, and the data matrix was 128 × 128. The echo time to the centre of *k*-space was 35 msec. For the PGSE sequence, the pulsed gradient lobes were 18.4 msec long (δ) with 60 msec between the two leading edges (Δ), and a rise time of 2 msec (τ), giving a spin echo time (TE) of 115 msec (Fig. 1). The imaging gradients were rephased during diffusion encoding to eliminate cross terms between the applied gradients. The diffusion sensitivity parameters (b values) were altered by varying the gradient amplitude (G). Two images were collected with each of the following, relatively low, b values: 0, 0.2, 3, 15, 47, 80, 115, 206, 246, 346, 468 sec/mm^2 and with a repetition time (TR) of 10 sec, giving a total imaging time of 220 sec for the IVIM measurement. If, during acquisition, it was observed that any image was obviously affected by motion (resulting in large areas of signal attenuation on the modulus image), additional images were acquired at the appropriate b values. This generally occurred for one or two images per subject.

Generally (13),

$$b = \gamma^2 \int_0^t \left| \int_0^{t'} G(t'')\, dt'' \right|^2 dt' \qquad [1]$$

where G(t") is the pulsed magnetic field gradient and t represents the time taken to form a gradient echo. Thus, for trapezoidal gradients, b was calculated to be:

$$b = \gamma^2 G^2 \left[\frac{2}{3}\left(\delta + \frac{3\tau}{2}\right)^3 - \frac{43\tau^3}{60} - \frac{2\delta\tau^2}{3} + (\delta + \tau)^2(\Delta - \delta - 2\tau) \right] \qquad [2]$$

By including the rise time in this calculation, the diffusion sensitivity parameter is reduced by 16%.

Analysis

Gross maternal or fetal movement results in very obvious, large areas of severe signal attenuation on the raw modulus images. If the signal resulting from these images is sampled, it lies well outside the range of the other data points collected at similar b-values. All images were checked prior to analysis, and those on which bulk motion was apparent were discarded. If motion had been observed during acquisition, so that an additional image had been acquired at that b value, data from this image was substituted.

The average signal from a region of interest (ROI) lying over the placenta in each image was measured. The ROI was chosen to be as large as possible, typically containing 100 pixels, but excluded any obvious blood vessels or artefacts. Blood vessels were identified by averaging together each set of images; vessels had a lower intensity on the resulting image since the signal arising from the blood vessels was attenuated at lower pulsed gradients (Fig. 2). f, D, and D* were determined by fitting (14) the following bi-exponential expression to the averaged ROI signals:

$$S(b) = S_0[(1 - f)e^{-bD} + fe^{-bD^*}] \qquad [3]$$

where S(b) represents the signal intensity and S_o is the signal intensity when b = 0. A typical plot of the data and the fitted curve is displayed in Fig. 3. The data were corrected for the effect of noise in low signal modulus images (15) by using a lookup table within the fitting program. Graphs were plotted of the fitted f, D, and D* against gestational age, and the mean and standard deviation for all normal healthy pregnancies were calculated.

Subject Movement

The PGSE sequence is very sensitive to subject motion within the diffusion encoding period. Larger fetal movements lead to artificially high signal attenuation in the

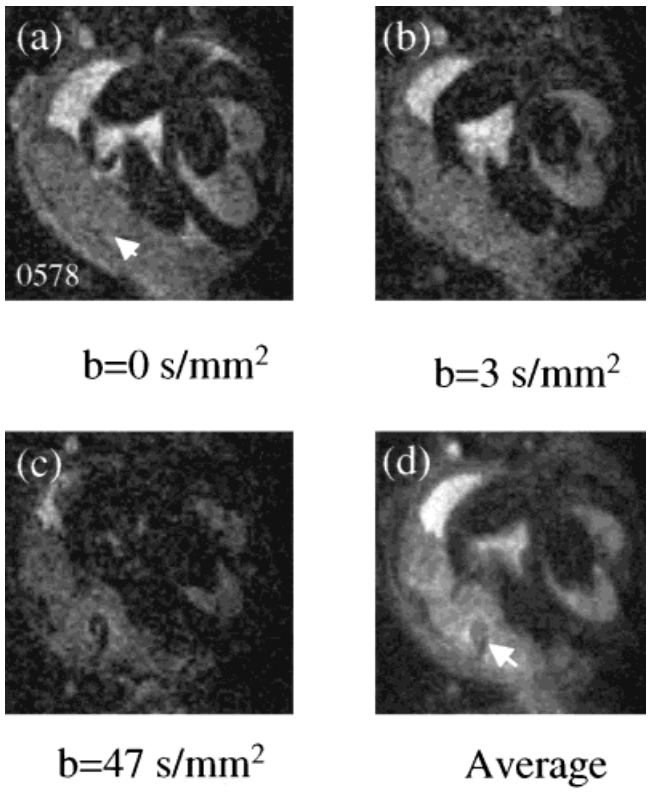

FIG. 2. Images obtained using the PGSE sequence. **a**, **b**, **c:** Images obtained with diffusion sensitivity parameters 0, 3, and 47 sec/mm^2, respectively. **d:** In the averaged image, blood vessels appear darker and are marked with an arrow. This region is also marked on image **a** where no visible change in signal is apparent.

placenta, the fetal tissues and in the amniotic fluid. Images obviously affected in this way were simply discarded from further analysis. The problem arising from less dramatic fetal movements has been examined experimentally. This type of movement would attenuate signal from the placenta in a similar, but smaller, way to more dramatic movement events. One pregnant patient was scanned continuously to obtain 5 measurements of f, D, and D*.

EXPERIMENTAL RESULTS

Figure 4a, b, and c show the variation in the fitted parameters with gestational age. The value of f averaged over all normal healthy subjects was found to be 26 ± 6 % (mean ± SD), and a weak trend with gestational age was found indicating that f decreased at the rate of 0.6% per week ($P = 0.05$, single-factor ANOVA). The value of D averaged over all normal healthy subjects was $1.7 \pm 0.5 \times 10^{-3}$ mm^2/sec and of D* was $57 \pm 41 \times 10^{-3}$ mm^2/sec.

Movement Results

For the 5 repeated measurements on one subject, only one of the 130 images collected was considered to be affected by gross fetal movements from a large area of signal attenuation visible on the image. Figure 5a shows all the diffusion attenuation data sets including the point from the affected image (marked as a diamond): it clearly lies well away from the rest of the data.

Coherent motion across the whole voxel where by each spin moves at the same velocity, results in a signal phase shift, which is not detected in modulus images. Rotational and warping movement, where by spins move at different velocities within a voxel, causes the spins to dephase and results in signal attenuation. Given the unpredictable nature of fetal motion, it is assumed that the amount of motion is not identical during each image acquisition. Therefore, the amount of dephasing would vary from image to image. As the b-value is increased, the sequence becomes more sensitive to this type of movement. The extent of rotational movement would be reflected by an increase in the standard deviation in signal intensities with increasing b value. The SD at each b-value was calculated, normalized, and plotted against diffusion sensitivity in Fig. 5b. The SD remained fairly constant with increasing diffusion sensitivity ($r = 0.66$).

Optimization Method

The signals measured following the PGSE sequence are inevitably affected by noise, which will be assumed to be normally distributed. This noise propagates through the analysis so that the fitted values of f, D, and D* are distributed about the true values. The width of the distribution in the fitted parameters is defined by a confidence interval of plus or minus one standard deviation, and is related to the exact choice of b-values at which the signals are sampled. The choice of b-values was optimized to minimize this confidence interval. The alpha matrix (14) defined in Eq. [4] where the terms represent the differentials of Eq. [3] with respect to S_o, f, D, or D* in turn, and the expression is summed over N values of b. ϕ is the experimentally measured image signal to noise ratio, expressed as a percentage.

$$\alpha_{kl} = \sum_{i=1}^{N} \frac{1}{\phi^2} \left[\frac{\partial S(b_i;a)}{\partial a_k} \frac{\partial S(b_i;a)}{\partial a_l} \right] \qquad [4]$$

The covariance matrix (14)

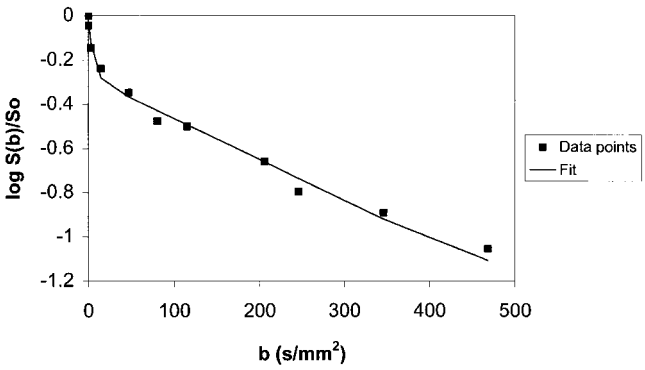

FIG. 3. A typical plot of the signal attenuation versus diffusion sensitivity parameter, b. Note the obvious bi-exponential nature of the data on this log/lin plot.

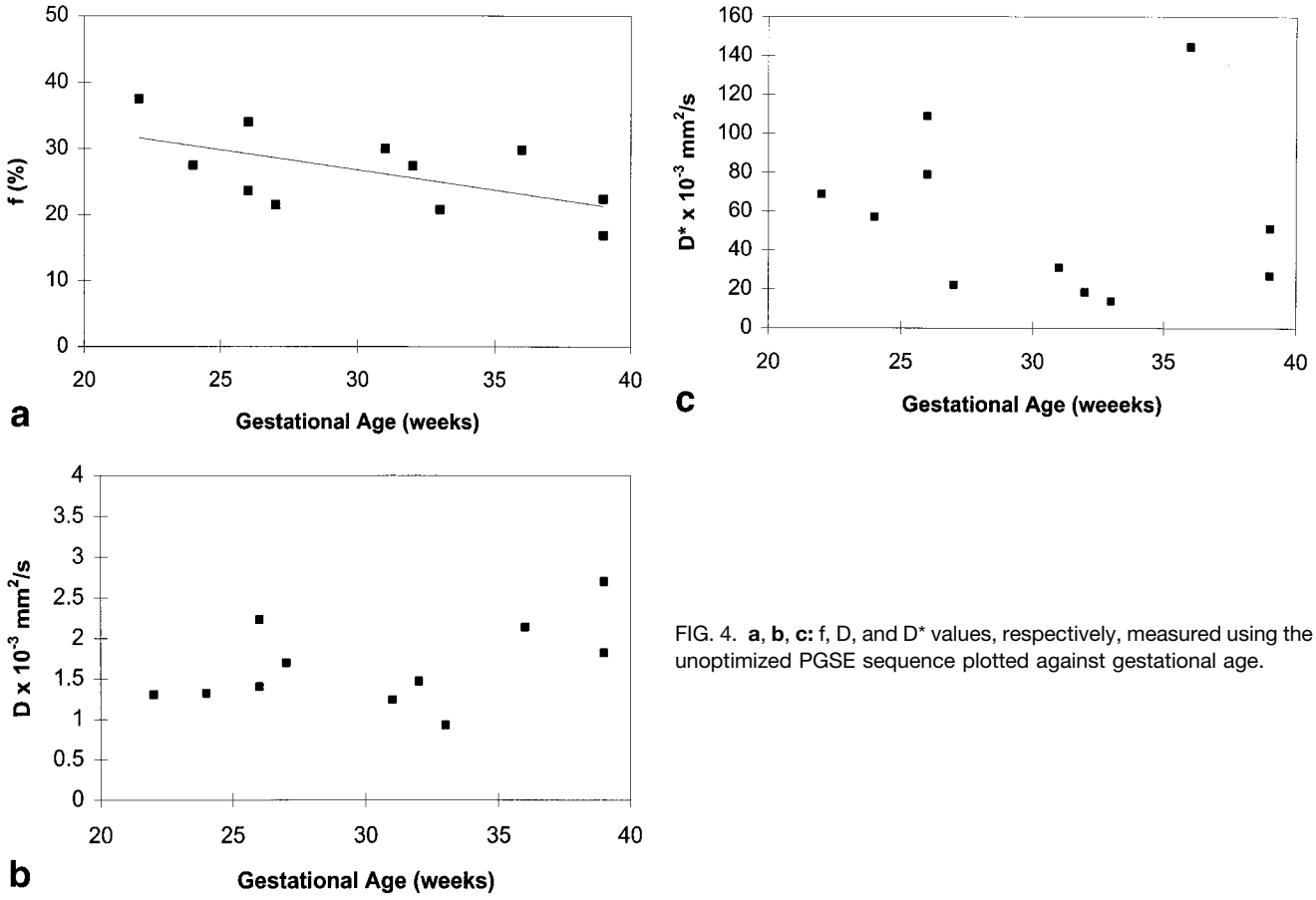

FIG. 4. **a**, **b**, **c:** f, D, and D* values, respectively, measured using the unoptimized PGSE sequence plotted against gestational age.

$$[C] \equiv [\alpha]^{-1} \quad [5]$$

was calculated as an estimate of the standard errors in the fitted parameters. The values of S_o, f, D, and D* obtained *in-vivo*, were then substituted into the covariance matrix and used to determine the percentage confidence limits σS_o, σf, σD, and σD*,

$$\sigma a_1 = \pm \sqrt{\Delta\chi^2}\ \sqrt{C_{11}} \quad [6]$$

where $\Delta\chi^2$ is the tabulated value corresponding to a desired confidence level of 68% for four degrees of freedom (14). The error in fitting each parameter was then calculated separately as $\sigma S_o/S_o\%$, σf/f%, σD/D%, and σD*/D%*.

The initial aim of this optimization was to minimize the value of σf/f%, σD/D%, and σD*/D*% with respect to the selection of b values for a fixed imaging time. Two different schemes were investigated for distributing the b values: linear [a, $2a$, $3a$, . . ., na] and geometric [a, (ar), (ar^2), (ar^3), . . ., $ar^{(n-1)}$]. TR was fixed at 10 sec to allow full recovery after the spin echo. By reducing TR, a greater number of images could be acquired within the total experimental time, and TR could be optimized separately to improve signal to noise per unit time, but this would have no effect on optimum b-value scheme. It was fixed here at 10 sec to minimize any spin history effects. The image signal-to-noise ratio was experimentally measured at 20:1.

Firstly, the geometric sampling scheme was investigated by using different combinations of a and r to alter the b-values. Keeping the total acquisition time constant, the number of samples and the number of times each sample was acquired, were varied. This was then repeated for total acquisition times ranging from 100 to 3600 sec.

For the linear scheme the total imaging time was initially fixed and a was varied. Then the optimum number of samples and the number of repeats at each b value were investigated. Again, this was repeated for total acquisition times ranging from 100 to 3600 sec.

It became apparent that σD*/D*% far exceeded σf/f% and σD/D%. Consequently, the values obtained for σf/f% and σD/D% at each combination of a and r, were summed with even weighting to produce a confidence measure, which shall be referred to as $C_{f,D}$ for the purposes of this paper. Geometric and linear optimizations were then repeated with the aim of reducing $C_{f,D}$ to less than 15% for a minimum acquisition time, i.e., the final optimization of the sequence excluded D*, as measurements of D* were found to be too noisy to be useful.

Optimization Results

Figure 6 shows a contour plot of the confidence measures for the geometric sampling scheme as a and r were varied. The total acquisition time was fixed at 800 sec (16 values of b, each repeated 5 times). As expected, it was found that

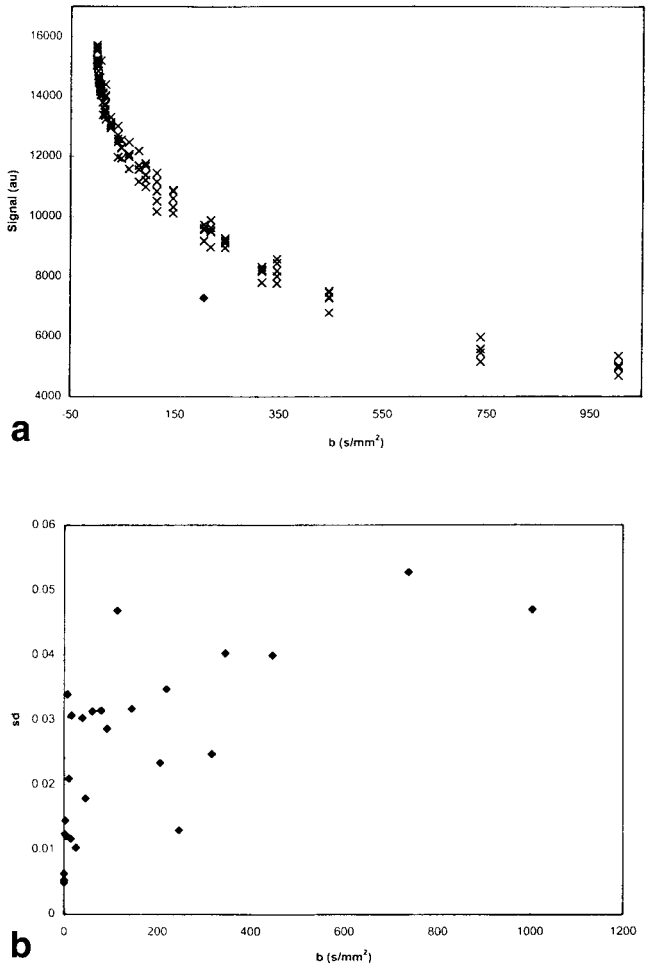

FIG. 5. **a:** The signal collected from 131 placental images collected at various b-values. The data point effected by stochastic fetal motion is marked with a diamond. **b:** SD of the normalized image signal for a placental ROI at each b-value.

the minimization of σD*/D*% required the greatest concentration of image acquisitions to be at lower b-values. Conversely, the minimization of σD/D% required the greatest concentration of image acquisitions to be at higher b-values. The minimization of σf/f% lay between these two extremes. This was a general result for all sampling schemes. As indicated above, it was also apparent that measurements of f and D were far more reproducible than D* measurements, illustrating the inherent insensitivity of the PGSE sequence to D*, even in the presence of a large volume of moving blood (f) as found in the placenta. For 16 sample points, the optimum sampling scheme was found when $r = 1.53$ and $a = 2.00$. This may be compared to the optimized sampling scheme with the same total imaging time used in the initial experiment. Details of these results are found in Table 1 and illustrate that the main contribution to the total experimental accuracy is the total imaging time.

As expected, if the total acquisition time was permitted to change, the optimum combination was the same irrespective of the number of times the sampling scheme was repeated. Figure 7 is a plot of the confidence measure $C_{f,D}$ against total acquisition time. The number of b-values was fixed at 16 (square points) (using the optimum sampling scheme; i.e., geometric with $r = 1.53$, $a = 2.00$) and the total acquisition time was varied by increasing the number of repeats of each sample point. As the total scanning time increased, a diminishing improvement in $C_{f,D}$ was obtained as expected. If the PGSE sequence could be applied with this TR for 1 hour, $C_{f,D}$ would be reduced to 6.8% for an image signal-to-noise ratio of 20:1. To reduce $C_{f,D}$ to less than 15%, 5 repeats were necessary. Figure 7 also plots the value of $C_{f,D}$ against total acquisition time when the number of b-values was fixed at 24 (circular points) (using the optimum sampling scheme; i.e., geometric with $r = 1.31$, $a = 2.25$). It is apparent that the value of $C_{f,D}$ did not vary significantly with the number of b-values used in this range and was mainly dependent on the total acquisition time.

Figure 8 displays the variation in $C_{f,D}$ using the linear sampling scheme. For a fixed time of 800 sec (16 samples, 5 repeats) the minimum $C_{f,D}$ was calculated at 15.9%. This compares to the value of 14.9% when using the geometric scheme (16 sample points, $r = 1.53$ and $a = 2.00$).

The error in fitting each parameter was also calculated for the b-values used in the experimental section of this paper. These values are displayed in Table 1 together with the summary of the above results.

DISCUSSION

Intravoxel incoherent motion analysis provides a noninvasive method of assessing f and D to provide information about the movement of blood in the placenta. The voxel volume is relatively large and the distribution of velocities present within the feeding and draining vessels, and their

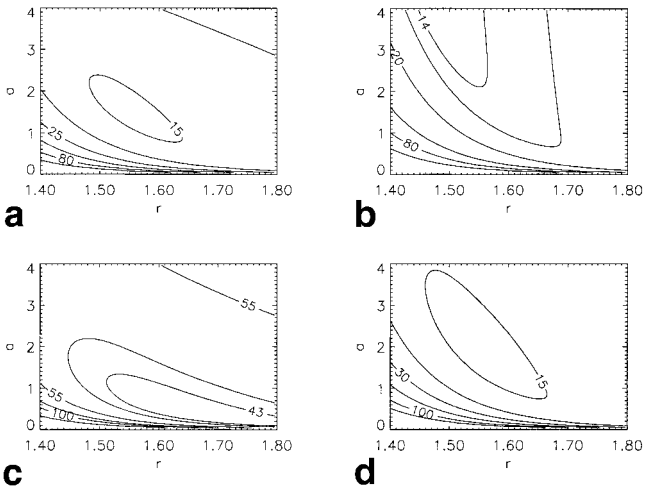

FIG. 6. A contour plot of the variation in fitting errors for each parameter using the geometric sampling scheme using 16 samples and 5 repeats. **a:** The variation in σf/f% as *a* and *r* are varied. Contours are drawn at 15, 18, 25, 40, 80, 200 units. **b:** The variation in σD/D% as *a* and *r* are varied. Contours are drawn at 14, 15, 20, 40, 80, 200 units. **c:** The variation in σD*/D*% as *a* and *r* are varied. Contours are drawn at 43, 45, 55, 75, 100, 200 units. **d:** The variation in $C_{f,D}$ as *a* and *r* are varied. Contours are drawn at 15, 20, 30, 50, 100, 200 units.

Table 1
Summary of the Optimization Results

	f %	D 10^{-3} mm^2/s	D* 10^{-3} mm^2/s	b-Values (geometric scheme) a	r	N^0 Samples	N^0 Repeats	Time (s)	Confidence measure σf/f %	σD/D %	σD*/D* %
optimized for 220s	26	1.7	57	1.9	1.86	11	2	220	28.1	27	83.6
optimized for C_{Df} = 15%				2	1.53	16	5	800	14.86	14.24	44.9
unoptimized				0, 0.2, 3, 15, 47, 80, 115, 206, 246, 346, 468				220	29.2	33.8	86.5

orientations are very varied. Therefore it is expected that the contributions from these vessels are dephased by even the lowest amplitude of pulsed gradients and do not contribute significantly to the measured value of D or D*. Fetal blood within the placenta is transported through a vascular bed with a hierarchy of vessel sizes, the smallest of which are hairpin like capillary loops which carry blood in a random walk. A large fraction of the placenta is filled with maternal blood in intervillous spaces that have constantly altering sizes and shapes. Both maternal and fetal blood flows, which are controlled by very different mechanisms of circulation, contribute to the value of f, D, and D* measured.

D*, which dominates at the lower values of b, relates to the circulation of blood on a scale that is smaller than a single voxel. This parameter may be related to the rate of perfusion in the placenta which has also been measured using the nonselective/selective inversion recovery sequence to produce perfusion maps (5). A large degree of variability in D* was expected, due to the value of σD*/D*% calculated for the unoptimized sequence. However, a striking feature of the results obtained with the spin labeling technique is the spread in perfusion rate across the placenta. Therefore, it is likely that some of the variation in the results obtained using ROI data is due to the biological differences between subjects and heterogeneity in the structure of the placenta, despite the fact that regions were always chosen to avoid areas that apparently corresponded to vessels. Nonetheless, with the S/N currently available, D* measurements are too noisy to be useful.

Diffusion measurements are also sensitive to background gradients and in the placenta there may be considerable local susceptibility gradients. Future work will be aimed at implementing diffusion sequence with no sensitivity to background gradients (16), although it may only be possible to implement these in a model (remotely perfused) placenta system because of the increased gradient strength required.

Another source of variability would be the orientation of the placenta with respect to the axis along which the pulsed gradients were applied, because it has become clear that the placenta is a heterogeneous, but structured organ. In future work the orientation of the gradients with respect to the placenta will be standardized.

The additional data acquired to examine the effect of fetal motion on the data indicates that this effect does not dominate over other sources of variability including noise in the fit and the pulsatile nature of placental blood flow.

Values of D*, as quoted in the literature (17,18) are 6.5×10^{-3} and 80×10^{-3} mm^2/sec for the cat and rat brain, respectively. The value measured here for the placenta is (57×10^{-3} mm^2/sec). Although comparisons have limited usefulness, as the data was collected with different sequence parameters and D* is very sensitive to noise in the fit, the results are strikingly different. In the brain, D* relates to the velocity of circulating blood and the length of the capillary limb (4) within pseudo-randomly orientated blood vessels. This interpretation is analogous for the fetal

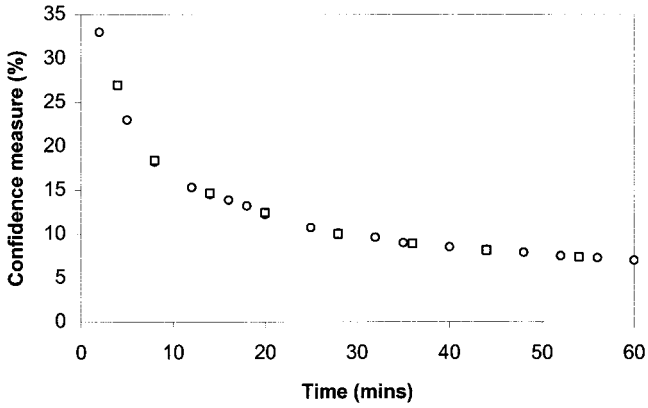

FIG. 7. Plots the decreasing value of the confidence measure $C_{f,D}$ as it relates to the total scanning time with the geometric sampling scheme. The number of values of b was fixed at 16(□) and 24 (○).

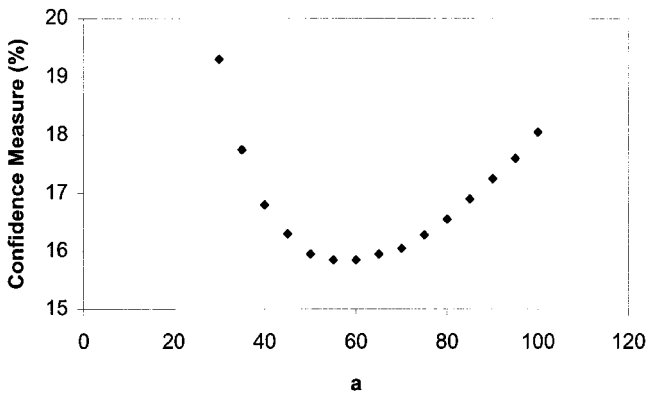

FIG. 8. Plots the variation in $C_{f,D}$ with *a* using the linear sampling scheme. There are 16 samples repeated 5 times.

vascular system, however, the maternal blood does not travel in capillaries through the placenta, but collects in pools in the intervillous spaces. In the placenta, the PGSE sequence measures a D* value that probably relates to the movement of blood in the intervillous spaces and the flow of blood in the fetal capillaries within the villi.

The value of D is related to molecular mobility on a smaller scale, which is governed by random Brownian motion and therefore the physical characteristics of the tissue, such as cell size and membrane permeability. This value showed no trend with gestational age as measured with the unoptimized sequence. In the normal cat and rat brain (17,18) D was found to be 0.72×10^{-3} and 0.8×10^{-3} mm^2s^{-1}, respectively, whereas a mean value of 1.7×10^{-3} mm^2s^{-1} was measured here. This difference is likely to be due to the large intracellular spaces found in the placenta (19) compared with the brain.

The value of f measures the fraction of blood flowing in the voxel compared to the total voxel volume. A weak trend was found whereby f decreased at 0.6% per week with gestational age. The fractional volume of intervillous space, relative to the total villous and intervillous volumes has been reported to vary as follows: 0.56 at 13–15 weeks, 0.48 at 22–23 weeks, 0.54 at 29–31 weeks, and 0.46 at 36–39 weeks (19) and therefore a decrease in f with gestational age might be expected. Typical values of f in the cat and rat brain (17,18) are 8.3 and 5%, which is far less than the value measured for the placenta (26%). Although the usefulness of direct comparisons is again limited by the differences in the sequence parameters, this difference is to be expected due to the larger fractional volume of the intervillous spaces in the placenta compared to the intravascular space of the brain, which is 5% of the total brain volume (20). Because of this difference, values of f are more accurate when measured in the placenta.

The optimum sequence for measuring IVIM in the placenta was found to have 16 b-values, geometrically spaced with $r = 1.53$ and $a = 2$. If applied for 800 sec, $\sigma f/f = 14.86\%$, $\sigma D/D = 14.24\%$, $\sigma D^*/D^* = 44.9\%$. For simplicity of optimization and implementation, the optimization has only considered general systematically varying values of b. Therefore, it is possible that other schemes for arranging b-values will further decrease the level of noise in the fit. It is important to note that the optimization was performed for a basic image signal-to-noise of 20:1, which is typical for whole-body EPI at 0.5 T. At lower noise levels, the sensitivity of the sequence improves dramatically (see Pekar, Ref. 8), although it is expected that the optimization results will remain the same and the values of $\sigma f/f$, $\sigma D/D$, and $\sigma D^*/D^*$ will scale. Furthermore, no attempt has been made to change TR. Mathematically, the optimization of TR is straightforward, but in practice may be empirical, being dependent on patient movement and spin history effects.

Safety is always an important issue when scanning fetuses. EPI causes low RF deposition but uses rapidly varying gradients, which give rise to relatively high magnetic field switching rates (dB/dt). The main risk from high magnetic field switching is cardiac defibrillation. However, in this implementation of EPI the switching rates (instantaneous maximum 19 T/sec), and switching times (sinusoidal period 850 μs), are much lower than those expected to pose any risk to the human heart (21). In the fetus the heart is surrounded by lungs filled with conducting amniotic fluid, contained in a pregnant abdomen, providing a potentially larger area around which circulating currents can form. However, because the fetal heart is always close to the centre of the magnet, when a transverse gradient is switched so that the gradient sign reverses across the volume of interest, the effective current loop radius and hence induced electric field are reduced. The minimal RF power deposition involved with EPI could be particularly important in the fetus where the dissipation of heat may be restricted as the fetal and maternal circulatory systems are separate.

CONCLUSION

This paper presents the first in vivo measurements of IVIM in the human placenta, and gives the range of f, D, and D* values to be expected in normal pregnancy. The optimization has shown that the values of D and f can be measured to a precision of 15% within 14 min, but higher signal-to-noise is required for precise measurement of D*. Using the unoptimized sequence a weak trend was found linking the value of the f to gestational age. Now that the PGSE sequence has been optimized, further work will include the collection of data from both the normal and compromised cases using the optimized sequence.

ACKNOWLEDGMENTS

We are grateful to the Medical Research Council for funding this work. We would like to thank Dr. R. Coxon and Ms. S. Al-Sahab for their assistance.

REFERENCES

1. Le Bihan D, Breton E, Lallemand D, Grenier P, .Cabanis E, Laval-Jeantet M. MR imaging of intravoxel incoherent motions: application to diffusion and perfusion in neurological disorders. Radiology 1986;161:401–407.
2. Le Bihan D, Breton E, Lallemand D, Aubin M, Vignaud J, Laval-Jeantet M. Separation of diffusion and perfusion in intravoxel incoherent motion MR imaging. Radiology 1998;168:497–505.
3. Henkelman RM. Does IVIM measure classical perfusion? Magn Reson Med 1990;16:470–475.
4. Le Bihan D, Turner R. The capillary network: a link between IVIM and classical perfusion. Magn Reson Med 1992;27:171–178.
5. Francis ST, Duncan KR, Moore RJ, Baker PN, Johnson IR, Gowland PA. Noninvasive mapping of placental perfusion. Lancet 1998;351:1397.
6. Niendorf T, Dijkuizen RM, Norris DG, van Lookeren Campagne M, Nicolay K. Biexponential diffusion attenuation in various states of brain tissue: implications for diffusion-weighted imaging. Magn Reson Med 1996;36:847–857.
7. Stejskal EO, Tanner JE. The use of spin-echos in a pulsed magnetic field gradient to study anisotropic, restricted diffusion and flow. J Chem Phys 1965;43:3597–3606.
8. Pekar J, Moonen CTW, Van Zijl PCM. On the precision of diffusion/perfusion imaging by gradient sensitization. Magn Reson Med 1992;23:122–129.
9. Mansfield P, Stehling MK, Ordidge R. Echo-planar imaging of the human fetus in utero at 0.5 T. Br J Radiol 1990;63:833–841.
10. Roberts N, Garden AS, Cruz Olive LM, Whitehouse GH, Edwards RH. The estimation of fetal volume by MRI and stereology. Br J Radiol 1994;67(803):1067–1077.
11. Levine D, Hatabu H, Gao J, Atkinson MW, Edelman RR. Fetal anatomy with fast MR sequences. Am J Roent 1996;167:905–908.

12. Baker PN, Johnson IR, Gowland PA, Hykin J, Harvey PR, Freeman A, Adams V, Worthington BS, Mansfield P. Fetal weight estimation by echo-planar magnetic resonance imaging. Lancet 1994;343:644–645.
13. Ahn CB, Cho ZH. A generalized formulation of diffusion effects in μm resolution nuclear magnetic resonance imaging. Med Phys 1989;16:22–28.
14. Press WH, Teukolsky SA, Vetterling WT, Flannery BP. Numerical recipes in Fortran. Cambridge: Cambridge University Press; 1992. p 692–697.
15. Henkleman RM. Measurement of signal intensities in the presence on noise in MR images. Med Phys 1985;12:232–233.
16. Hong X, Dixon WT. Measuring diffusion in inhomogenous systems in imaging mode using antisymetric sensitising gradients. J Magn Reson 1992;99:561–570.
17. Le Bihan D, Moonen CTW, Van Zijl PCM, Pekar J, Despres D. Measuring random microscopic motion of water in tissues with MR imaging: a cat brain study. J Comput Assist Tomogr 1991;15:19–25.
18. Neil JJ, Bosch CS, Ackerman JJH. An evaluation of the sensitivity of the IVIM method of blood flow measurements to changes in cerebral blood flow. Magn Reson Med 1994;32:60–65.
19. Mayhew TM, Wadrop E. Placental morphogenesis and the star volumes of villous trees and intervillous pores. Placenta 1994;15:209–217.
20. Weiss HR, Buchweitz E, Murtha TJ, Auletta M. Quanititative regional determination of morphometric indices of the total and perfused capillary network in the rat brain. Circ Res 1982;5:454–503.
21. National Radiological Protection Board. Her Majesty's Stationary Office (HMSO). Vol. 2(1). Didcot, England: Chilton, 1991.